Transactions, SMiRT-25
Charlotte, NC, USA, August 4-9, 2019
Division IV

ESTIMATION OF MEGATHRUST EARTHQUAKE SOURCE CHARACTERISTICS: ANALYSIS OF THE 1985 MEXICO AND 2015 CHILE EARTHQUAKES

Tetsuro Sasaki[1], Tetsumi Watanabe[2], Naoya Ishikawa[2], Yoshiho Kawai[2], Yusuke Tomozawa[3], Kenichi Kato[3], and Koichi Yabuuchi[4]

[1] Chubu Electric Power Co., Inc., Aichi, Japan (Sasaki.Tetsurou@chuden.co.jp)
[2] Chubu Electric Power Co., Inc., Aichi, Japan
[3] Kobori Research Complex, Inc., Tokyo, Japan
[4] Kajima Corporation, Tokyo, Japan

ABSTRACT

Precise predictions of earthquake ground motion are pivotal in the effective seismic design of key infrastructure in seismically active regions. The Hamaoka nuclear power plant, Japan, is located above the source region of the Nankai Trough megathrust earthquake. However, one of the significant issues is that the megathrust earthquake source characteristics are poorly constrained due to limited observations. Therefore, we analyzed the strong-motion records of the Mexico and Chile megathrust earthquake, similar to the Nankai Trough megathrust earthquake source region. The 19 September 1985 Michoacan Mexico earthquake (M_W 8.0) and the 16 September 2015 Illapel Chile earthquake (M_W 8.3) were megathrust earthquakes with a number of seismic records acquired above both source regions. We estimated the source spectra, Q values, and site amplification factors via spectral inversion analysis. We then estimated the short-period amplitude level and stress drop from the source spectra. The short-period amplitude level is an important parameter that affects strong ground motion predictions. The relationship between seismic moment and short-period amplitude level was comparable to a conventional study. The stress drop exhibited a slight focal depth dependency, although the variation was large.

INTRODUCTION

For the seismic design of important facilities, it is important to predict earthquake ground motion precisely. The Hamaoka nuclear power plant is located above the source region of the Nankai Trough megathrust earthquake at subduction zone. One of the significant issues is source characteristics of megathrust earthquakes occurred just under observation points.

The Nankai Trough megathrust earthquake at subduction zone is the major concern for Japan but there are not enough observed strong motion records in this region. Therefore, in order to investigate megathrust earthquakes, we collected the strong motion records observed at both Mexico and Chile regions. In these regions, megathrust earthquakes were occurred just under observation points similarly to Nankai Trough.

We analysis the relationship between seismic moment and the amplitude of the acceleration source spectral level (short-period level). Here, the short-period level is the flat level of the acceleration source

spectrum. The relation between depth and stress drop is also discussed. These parameters were estimated by spectral inversion method using the strong ground motion records.

DATA SETS

Seismic records from the Mexico region were downloaded from Consortium of Organizations for Strong-Motion Observation Systems (COSMOS). Only records near the source area of the 1985 Mexico earthquake were selected (Figure 1(a) and Table 1(a)). The mainshock fault plane of Mendoza and Hartzell (1989) and the largest aftershock fault plane of Mendoza (1993) are shown in Figure 1(a) to highlight the locations of the source areas relative to the analyzed earthquakes. The focal mechanism solutions are taken from the Global CMT Project. Twenty-one additional earthquakes were selected for the analysis (N_{eq}), including eight interplate earthquakes. We classified the analyzed earthquakes as plate boundary earthquakes and other earthquakes because data from the interplate earthquakes were limited. Earthquakes near the plate boundary are shown in red in Figure 1(a), and the other earthquakes are shown in blue. A peak ground acceleration (PGA) of ≤200 cm/s^2 was used to avoid the influence of nonlinear ground motion. A total of 100 seismic records (N_{obs}) from 20 seismic stations (N_{site}) were analyzed. The earthquakes were M_w 5.2–7.2 events that were located 13–200 km from the seismic stations.

Strong-motion records from the Chile region were downloaded from Centro Sismológico Nacional (CSN; http://evtdb.csn.uchile.cl/). Only records near the source area of the 2015 Chile earthquake were selected (Figure 1(b) and Table 1(b)). The mainshock fault plane of Okuwaki et al. (2016) is shown in Figure 1(b) to highlight the location of the source area relative to the analyzed earthquakes. We analyzed an additional 31 earthquakes (all interplate earthquakes) from 27 seismic stations, using a total of 386 seismic records (PGA ≤ 200 cm/s^2). The earthquakes were M_W 5.0–7.0 events that were located 24–200 km from the seismic stations. Several proximal seismic records were included in the data set because the interplate earthquakes occurred beneath the continental area.

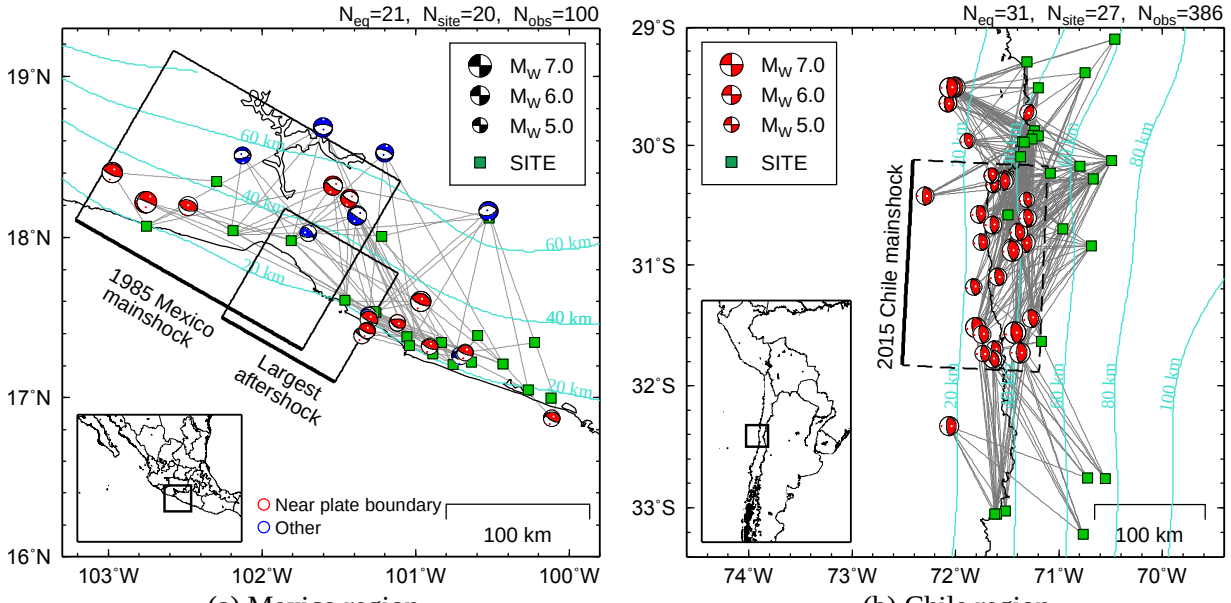

(a) Mexico region (b) Chile region

Figure 1. Analyzed data sets for the (a) Mexico and (b) Chile regions. The colored beach balls are the focal mechanism solutions of the selected events, with their locations indicating the epicenters, and the green squares are the seismic stations used in the analysis. The gray lines indicate the station records that were used for each event. The rectangles mark the inferred rupture areas of the mainshock and the largest aftershock (Mexico region) events. The depth to the subduction interface is from Hayes et al. (2012).

Table 1. Earthquakes analyzed in this study

(a) Mexico region

USGS catalog					Type	Remarks
Date and time (UTC)	Lat. (deg.)	Lon. (deg.)	Depth (km)	M_w		
1985.09.19 13:17:47	18.190	-102.533	27.9	8.0	PB	Mainshock
1985.09.21 01:37:13	17.802	-101.647	30.8	7.6	PB	Largest aftershock
1986.04.30 07:07:18	18.404	-102.973	26.5	7.0	PB	
1990.05.11 23:43:50	17.282	-100.679	28.0	5.6	PB	
1990.05.31 07:35:27	17.260	-100.707	22.6	6.0	OP	
1991.01.14 21:11:04	18.029	-101.700	30.5	5.5	OP	
1992.03.31 20:56:37	17.469	-101.119	48.1	5.4	nPB	
1993.03.31 10:18:14	17.322	-100.910	29.5	5.5	PB	
1994.05.23 01:41:42	18.165	-100.527	55.3	6.3	OP	
1994.12.10 16:17:38	18.136	-101.384	48.1	6.5	OP	
1996.01.25 12:45:08	18.511	-102.129	76.5	5.5	OP	
1996.07.15 21:23:34	17.600	-100.965	18.3	6.8	PB	
1997.01.11 20:28:26	18.219	-102.756	33.0	7.2	nPB	
1997.05.22 07:50:53	18.684	-101.604	70.0	6.5	OP	
1998.04.20 22:59:14	18.525	-101.203	67.3	6.0	OP	
1998.05.09 17:03:12	17.519	-101.310	33.0	5.2	OP	
1998.07.11 05:21:13	17.390	-101.349	33.0	5.5	PB	
1999.06.21 17:43:04	18.324	-101.539	68.7	6.3	nPB	
1999.12.29 05:19:46	18.244	-101.432	69.9	5.9	nPB	
2000.08.09 11:41:47	18.198	-102.480	45.8	6.5	nPB	
2002.09.25 18:14:48	16.870	-100.113	5.5	5.3	PB	
2004.01.01 23:31:50	17.488	-101.303	29.4	6.1	PB	
2004.01.01 23:58:01	17.420	-101.315	28.3	5.7	PB	

(b) Chile region

USGS catalog					Type	Remarks
Date and time (UTC)	Lat. (deg.)	Lon. (deg.)	Depth (km)	M_w		
2015.09.16 22:54:32	-31.5729	-71.6744	22.4	8.3	PB	Mainshock
2013.10.31 23:03:59	-30.2921	-71.5215	27.0	6.6	PB	
2014.05.21 09:00:53	-30.4520	-71.3110	36.2	5.1	PB	
2015.08.12 00:14:40	-31.6968	-71.6227	30.0	5.5	PB	
2015.08.23 23:10:04	-29.7191	-71.2958	31.1	5.7	PB	
2015.09.16 23:18:41	-31.5622	-71.4262	28.4	7.0	PB	
2015.09.17 04:10:27	-31.5173	-71.8040	23.0	6.7	PB	
2015.09.17 20:40:31	-29.9614	-71.8851	5.7	5.5	PB	
2015.09.19 05:06:47	-29.6411	-72.0770	6.0	6.1	PB	
2015.09.19 09:07:09	-31.0999	-71.5902	28.0	5.7	PB	
2015.09.19 12:52:20	-32.3335	-72.0629	18.0	6.2	PB	
2015.09.20 03:02:02	-30.8468	-71.4623	45.5	5.0	PB	
2015.09.21 05:39:34	-31.5757	-71.7431	30.0	6.1	PB	
2015.09.21 17:40:00	-31.7275	-71.3792	35.0	6.6	PB	
2015.09.21 19:56:08	-31.7819	-71.6407	28.4	5.6	PB	
2015.09.22 07:13:00	-31.4441	-71.2653	58.0	6.0	PB	
2015.09.26 02:51:18	-30.8148	-71.3217	46.0	6.3	PB	
2015.10.03 06:26:55	-30.3010	-71.5510	38.0	5.9	PB	
2015.10.05 16:33:26	-30.3035	-71.5318	34.0	5.9	PB	
2015.10.09 18:27:36	-31.7323	-71.7325	35.0	5.5	PB	
2015.10.12 03:15:19	-31.1849	-71.8227	21.0	5.6	PB	
2015.11.07 07:31:43	-30.8796	-71.4519	46.0	6.8	PB	
2015.11.07 10:53:44	-30.7227	-71.3904	42.0	5.7	PB	
2015.11.11 01:54:38	-29.5067	-72.0068	12.0	6.9	PB	
2015.11.11 02:46:19	-29.5097	-72.0585	10.0	6.9	PB	
2015.11.21 23:05:30	-30.5754	-71.7676	27.0	5.8	PB	
2015.12.08 12:56:07	-30.8096	-71.7519	25.0	5.6	PB	
2015.12.19 19:25:05	-30.6053	-71.3057	48.3	5.8	PB	
2016.01.08 01:12:01	-30.6640	-71.6383	24.0	5.7	PB	
2016.01.29 20:07:15	-30.3325	-71.6327	35.8	5.2	PB	
2016.02.22 06:36:59	-30.4242	-72.2967	12.0	6.0	PB	
2016.03.12 16:05:15	-30.2495	-71.6502	36.8	5.1	PB	

PB: plate boundary earthquake; nPB: near plate boundary earthquake; OP: intraslab earthquake in the oceanic plate.

ANALYTICAL METHOD

The acceleration Fourier amplitude spectrum $F_{mn}(\omega)$ of a given seismic record is modeled in the spectrum inversion analysis via

$$F_{mn}(\omega) = \frac{\omega^2 R_{\theta\varphi} FS}{4\pi\rho\beta^3} \cdot S_m(\omega) \cdot \frac{1}{X_{mn}} \cdot \exp\left[-\frac{\omega X_{mn}}{2Q(\omega)\bar{\beta}}\right] \cdot \sqrt{\frac{\rho\beta}{\rho_r\beta_r}} \cdot G_n(\omega), \quad (1)$$

where m is the source (earthquake), n is the seismic station, $S_m(\omega)$ is the source characteristic of each earthquake, $G_n(\omega)$ represents the site amplification factors of each observation site, X_{mn} is the hypocentral distance, $R_{\theta\varphi}$ is the source radiation characteristic coefficient ($R_{\theta\varphi}$ = 0.63) [Boore and Boatwright, 1984], FS is amplification by the free surface (FS = 2), $\bar{\beta}$ is the average S-wave velocity of the propagation path ($\bar{\beta}$ = 3.7 km/s), and β and ρ are the source medium S-wave velocity and density, respectively. The medium β and ρ values at the reference site are β_r = 1.5 km/s and ρ_r= 2.2 g/cm^3, respectively.

The β and ρ values were set based on the source depth and were estimated using focal depths determined from the velocity structure in Mendoza et al. (1989) for the Mexico region and in Okuwaki et al. (2016) for the Chile region. Figure 2 shows the velocity models from these previous studies as well as the β and ρ values used in this study.

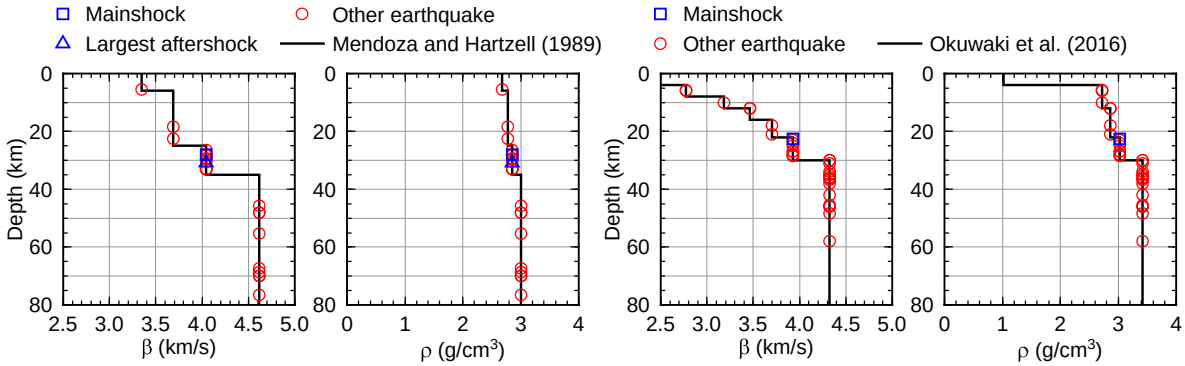

(a) Mexico region (b) Chile region

Figure 2. Velocity (β) and density (ρ) structure of the (a) Mexico and (b) Chile regions based on previous studies (black lines) and the values used in this study (red and blue symbols).

There is a trade-off between the source characteristics and the site amplification characteristics in the spectral inversion analysis, and constraints are needed to obtain a unique solution. This trade-off was resolved by assuming that the source spectrum of the medium and small earthquakes applies to the ω-squared spectrum instead of using the theoretical site amplification characteristics of the reference observation points as constraints [Kanaya et al., 2006]. The seismic moment was taken from the Global CMT Project. Only the corner frequencies (f_c) were used in the inversion. Furthermore, the target frequency was confined to the 0.2–5 Hz range.

The source spectra of the mainshock (Mexico and Chile) and the largest aftershock (Mexico) were evaluated by removing the site amplification and path characteristics of each modeled seismic record. We used the equivalent source distances (X_{eq}) to evaluate the fault model due to the large widths of the fault planes. Numerical data for the fault model were downloaded from the SRCMOD finite-source rupture model database.

The seismic records used in the evaluation of the mainshock source spectra consisted of records that satisfied the following criteria: $X_{eq} \leq 200$ km," "three-component PGA ≤ 200 cm/s^2," and seismic stations where the site amplification characteristics" were estimated. Seven and six stations met these criteria for the mainshock and the largest aftershock, respectively, in the Mexico region, and five stations met these criteria in the Chile region. We evaluated f_c by fitting an ω-squared spectrum to the estimated source spectrum. The stress drop $\Delta\sigma$ was calculated as (Brune, 1970)

$$\Delta\sigma = M_0 \left(\frac{f_C}{4.9 \cdot 10^6 \beta} \right)^3, \quad (2)$$

where M_0 is the seismic moment. The short-period level A was calculated as

$$A = 4\pi^2 {f_C}^2 M_0. \quad (3)$$

A is an important parameter that affects strong ground motion predictions.

RESULTS

The estimated Q values are shown in Figure 3. The estimated values are indicated by solid lines, with the standard error indicated by dashed lines. $Q(f) = 80f^{1.0}$ was estimated in the Mexico region. The standard error of the low-frequency region is larger than that of the high-frequency region, yielding a relatively lower estimation accuracy in the high-frequency region. There is no significant difference between the Q value of earthquakes near the plate boundary and the other earthquakes for $f > 1$ Hz. The Q values in the Chile region were slightly higher than those in the Mexico region, with $Q(f) = 200f^{0.8}$.

The source spectra of the estimated mainshocks and aftershock are shown in Figure 4 along with the result obtained by applying the ω-squared spectrum to the estimated source spectrum. The estimated source parameters of the large earthquakes are listed in Table 2. The f_C values of the large earthquakes may be evaluated at frequencies lower than the frequency range in the spectrum inversion analysis. Here, the seismic moment is fixed to the value provided by the Global CMT Project, and only f_C is fit to the data, with the constraint that it is confined to the 0.2–5 Hz range. This corresponds to the A estimation because the large-scale earthquake is defined by a region where the acceleration source spectrum is constant.

The relationship between M_0 and A is shown in Figure 5. The estimated A value of the 1985 Mexico earthquake is half that obtained from the empirical formula in Dan et al. (2001), which is estimated from previous variable-slip rupture models for crustal earthquakes around the world, whereas the estimated A value of the 2015 Chile earthquake corresponds to the average level.

The relationship between $\Delta\sigma$ and depth for each of the analyzed earthquakes is shown in Figure 6. The symbols indicate focal depth locations, with bars provided to define the extent of the fault planes for the large earthquakes. $\Delta\sigma$ tends to increase with depth, although the variation among the analyzed events is large.

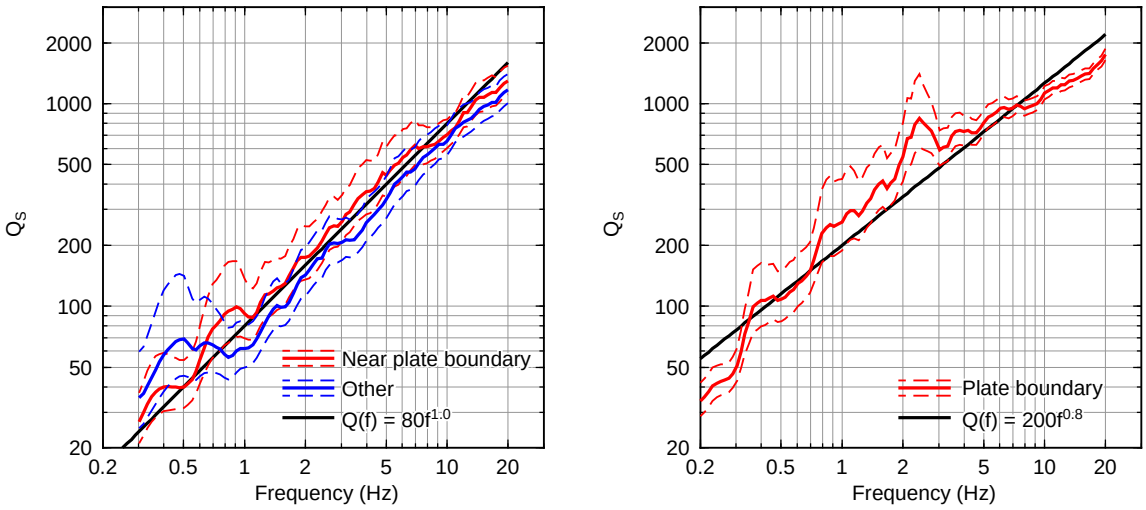

(a) Mexico region (b) Chile region

Figure 3. Estimated Q_S values.

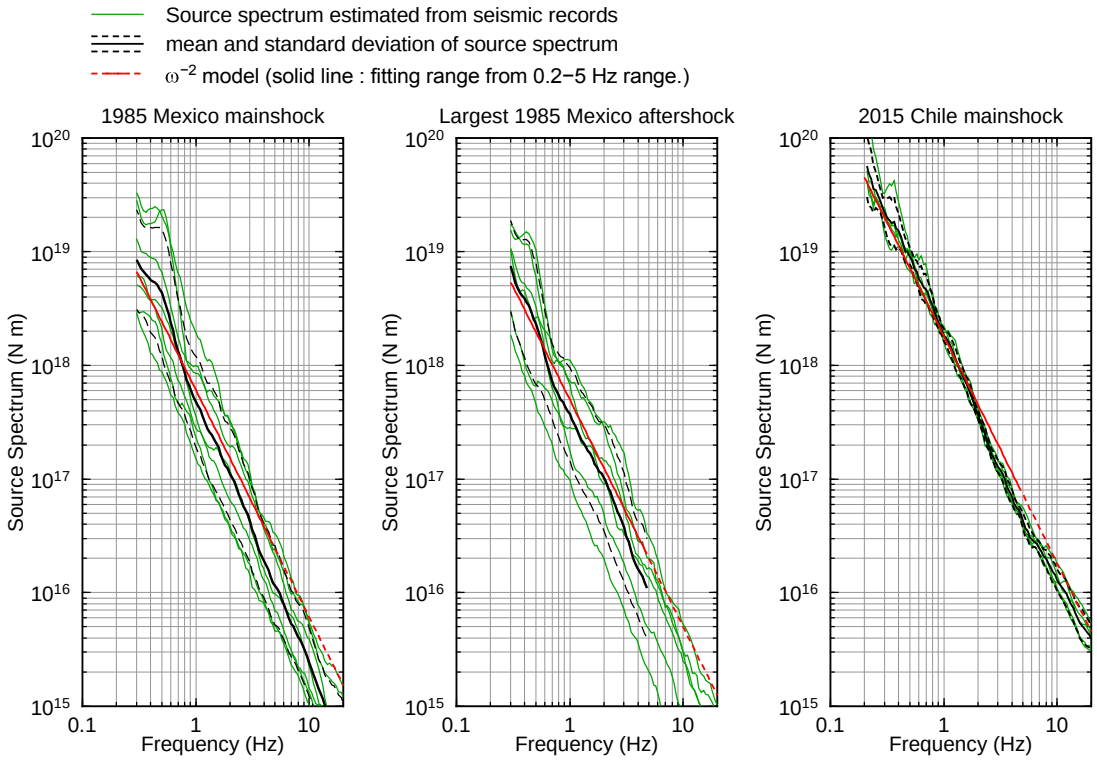

Figure 4. Estimated source spectra.

Table 2. Source parameters

	M_0 (N m)	f_C (Hz)	$\Delta\sigma$ (MPa)	A (dyne cm/s^2)
1985 Mexico mainshock	1.099×10^{21}	0.024	1.85	2.41×10^{26}
Largest 1985 Mexico aftershock	2.490×10^{20}	0.045	2.89	1.98×10^{26}
2015 Chile mainshock	3.229×10^{21}	0.024	6.04	7.18×10^{26}

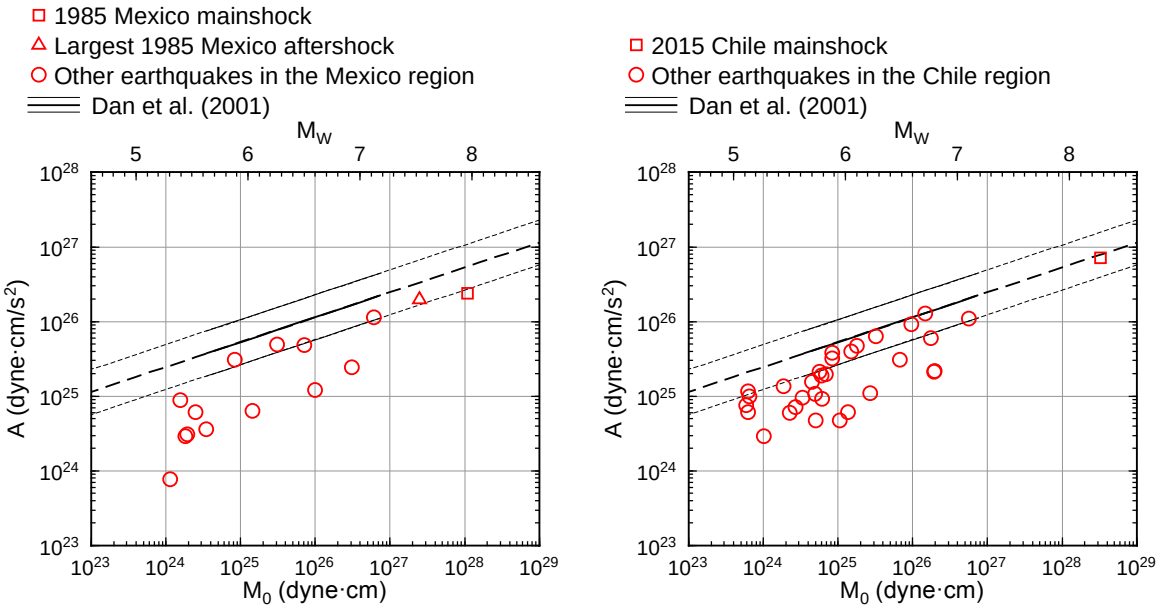

(a) Mexico region (b) Chile region

Figure 5. Seismic moment (M_0) versus short-period level (A). The mean, twice and half values are indicated by solid lines, with the extrapolation indicated by dashed lines.

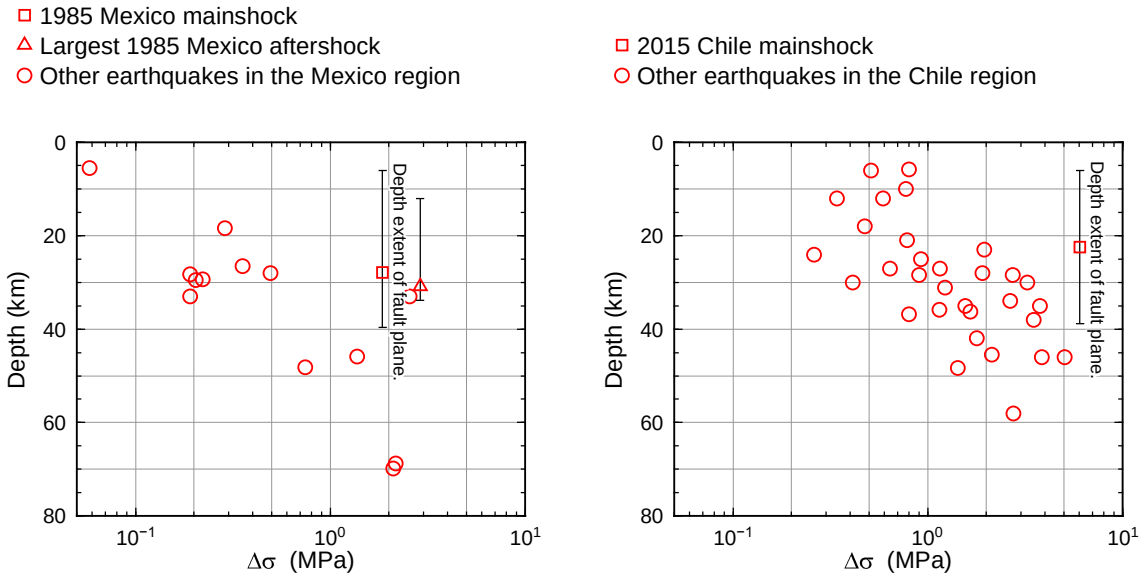

(a) Mexico region (b) Chile region

Figure 6. Stress drop ($\Delta\sigma$) versus depth.

CONCLUSION

A spectral inversion analysis was performed using strong ground motion records from the Mexico and Chile regions, and the path attenuation characteristics, Q values, source spectra, and site amplification factors were evaluated. We estimated the source parameters of the mainshock and the largest aftershock of the 1985 Mexico earthquake, and the mainshock of the 2015 Chile earthquake.

The estimated short-period level of the 1985 Mexico earthquake is half of the value estimated level obtained from the empirical formula in Dan et al. (2001), which is estimated from previous variable-slip rupture models for crustal earthquakes around the world, whereas that of the 2015 Chile earthquake corresponds to the average level. The stress drop tends to increase with depth in both regions, even though the variation is large.

REFERENCES

Boore, D.M. and J. Boatwright (1984). "Average Body-Wave Radiation Coefficients," *Bull. Seism. Soc. Am.*, Vol.74,1615-1621.

Brune, J. N. (1970). "Tectonic stress and the spectra of seismic shear waves from earthquakes," *J. Geophys. Res.*, Vol.75, 4997-5009.

COSMOS (Consortium of Organizations for Strong-Motion Observation Systems) http://db.cosmos-eq.org/scripts/default.plx

CSN (Centro Sismológico Nacional), http://evtdb.csn.uchile.cl/

Dan, K., Watanabe, M., Sato T., and Ishii, T. (2001). "Short-period source spectra inferred from variable-slip rupture models and modeling of earthquake fault for strong motion prediction," *J. Struct. Constr. Eng., AIJ*, 545, 51–62. (in Japanese)

Global CMT Project：http://www.globalcmt.org

Hayes, G.P., Wald, D.J., and Johnson, R.L. (2012). "Slab1.0: A three-dimensional model of global subduction zone geometries," *J. Geophys. Res*., Vol. 117.

Kanaya, J., Ikera, T., Hijikata, K. and Uetake, T. (2006). "Spectral inversion analysis based on strong motion records in Chuestu area of Niigata prefecture," *Summaries of Technical Papers of Annual Meeting, Architectural Institute of Japan*, B-2, 303-304. (in Japanese)

Mendoza, C., and Hartzell, S. H. (1989). "Slip Distribution of the 19 September 1985 Michoacan, Mexico, Earthquake - near-Source and Teleseismic Constraints," *Bull. Seis. Soc. Am*, 79 (3), 655-669.

Mendoza, C. (1993). "Coseismic Slip of 2 Large Mexican Earthquakes from Teleseismic Body Wave-Forms - Implications for Asperity Interaction in the Michoacan Plate Boundary Segment," *J. Geophys. Res.-Solid Earth*, 98 (B5):8197-8210.

Okuwaki R., Yagi, Y., Aránguiz, R., González, J. and González, G. (2016). "Rupture Process During the 2015 Illapel, Chile Earthquake: Zigzag-Along-Dip Rupture Episodes," *Pure and Applied Geophysics*, 173, 4, 1011-1020.

SRCMOD (Finite-Source Rupture Model Database): http://equake-rc.info/SRCMOD/